Synthesis and UV−Visible-Light Photoactivity of Noble-Metal−$SrTiO_3$ Composites

Vaidyanathan Subramanian,[†,‡,§] Ryan K. Roeder,[||] and Eduardo E. Wolf*[,†]

Department of Chemical and Biomolecular Engineering, Notre Dame Radiation Laboratory, and Department of Aerospace and Mechanical Engineering, University of Notre Dame, Notre Dame, Indiana 46556

The photocatalytic activity of strontium titanate ($SrTiO_3$) perovskite films has been examined and compared with that of commercially available titania (TiO_2, Degussa P25) in the degradation of a model pollutant, Victoria Blue dye. The effects of pH, synthesis temperature, and Sr/Ti ratio in the synthesis of the perovskite were examined. $SrTiO_3$ was prepared using Ag, Pt, or Au and characterized using optical and surface analysis methods. We found no clear evidence of substitution of the noble metal into the $SrTiO_3$ lattice, and most metal existed as zerovalent metal deposits. Addition of Ag to $SrTiO_3$ showed the most promising catalytic activity toward dye degradation. Degradation of the dye under UV−visible light was also observed to be enhanced only for Ag−$SrTiO_3$.

Introduction

Photocatalytic processes are environmentally friendly methods that utilize radiation energy to perform catalysis such as water splitting, waste mineralization, and recovery of precious metals.[1−3] The application of semiconductors, such as titania (TiO_2), as photocatalysts has been widely studied, but the application of perovskites as photocatalysts has been primarily studied to examine their water-splitting ability.[4−7] Perovskites, such as strontium titanate ($SrTiO_3$), have been used for water splitting because they provide a higher photopotential than TiO_2 and facilitate hydrogen and oxygen formation. Perovskites are also observed to be useful for the degradation of organic compounds in place of conventional photocatalysts, such as TiO_2.[8]

Perovskites have the general formula (ABO_3).[9] The perovskite structure provides the flexibility to vary the composition of the A and B sites and/or incorporate a combination of cations at the A and B sites to form substituted perovskites. In an ABO_3 perovskite, varying the stoichiometry or doping with a cation of a different valence state can, in principle, change the electronic properties.[10] Therefore, unlike TiO_2, one can control the composition and size of the constitutuent cations and can potentially alter the electronic structure of a perovskite semiconductor. Some typical general formulas of substituted perovskites are $A_xA'_{1-x}BO_3$, $AB_xB'_{1-x}O_3$, etc. Therefore, doping with different cations (A′ or B′) offers the potential to tailor the basic structure and hence the electronic and catalytic properties of substituted perovskites.

The focus of this work was on the perovskite $SrTiO_3$. $SrTiO_3$ has a cubic structure with a band gap (E_g) similar to that of TiO_2 ($E_g = 3.2$ eV).[9] Thus, $SrTiO_3$ alone is active only under UV radiation. The incorporation of a metal cation can alter the band structure of $SrTiO_3$ if the size of the doping metal ion is compatible with the lattice size of the perovskite. For example, Ag, Cr, Pt, Ru, and Ta have been incorporated into $SrTiO_3$ to promote water splitting.[6] Therefore, substitution of the Sr cation with a metal cation is expected to alter the band-gap characteristics, as it is known that an empty Ti 3d (t_{2g}) orbital contributes to the conduction band. Because photocatalysis in most semiconductors and TiO_2 involves absorption of UV photons (less than 3% of the solar spectrum) to excite electron−hole pairs, lowering the band gap (by preparing composites) can help in sensitizing $SrTiO_3$ to absorb light in the visible range and thus generate more charges to perform redox catalysis.

Therefore, the purpose of this study was to examine the following questions: (1) Can the stoichiometry (Sr/Ti) affect the photocatalytic activity of $SrTiO_3$? (2) Can doping with noble metals promote visible-light photocatalytic activity of $SrTiO_3$? To answer these questions, $SrTiO_3$ was synthesized with varying Sr/Ti ratio and Ag, Pt, or Au dopants using a modified Pechini process.[11] The photocatalytic activity of the catalyst was examined and compared with that of a commercial TiO_2 catalyst by monitoring the degradation of a common textile dye, Victoria Blue.

Experimental Section

Chemicals. Chemical reagents included hydrogen tetrachloroaureate(III) hydrate (>99.9%), hydrogen hexachlorplatinate-(IV) (99.9%), silver nitrate (99.999%), citric acid (anhydrous, >99.5%), ethylene glycol (>99%), titanium(IV) isopropoxide (99.999%), strontium acetate (99%), strontium carbonate (>99.9%), acid orange 7 (AO7), and Victoria Blue B (Aldrich Chemical Co.)

Synthesis of the Photocatalysts. Enhancement of the photocatalytic activity partly depends on the surface and deep trap states in a semiconductor.[12] One way to produce such states is to substitute metal ions of variable valence states that are capable of producing trap states for Sr and/or Ti in the $SrTiO_3$ lattice. Ion substitution depends on the technique used for synthesis of the composite catalyst. A modified Pechini process was used to provide intimate mixing between the precursor metal cations.[11] Moreover, the Pechini process also provided an option for introducing other metal dopants into the perovskite structure at the time of the complex formation. A solution of a TiO_2

* To whom correspondence should be addressed. Address: Department of Chemical and Biomolecular Engineering, University of Notre Dame, Notre Dame, IN 46556. E-mail: ewolf@nd.edu. Tel.: (574) 631 5897. Fax: (574) 631 8366.

† Department of Chemical and Biomolecular Engineering.

‡ Notre Dame Radiation Laboratory.

§ Present address: Roger Adams Laboratory, University of Illinois, Urbana-Champaign, IL 61801.

|| Department of Aerospace and Mechanical Engineering.

10.1021/ie050693y CCC: $33.50
Published on Web 01/11/2006

Scheme 1. Flowchart for the Synthesis of $SrTiO_3$ Catalysts

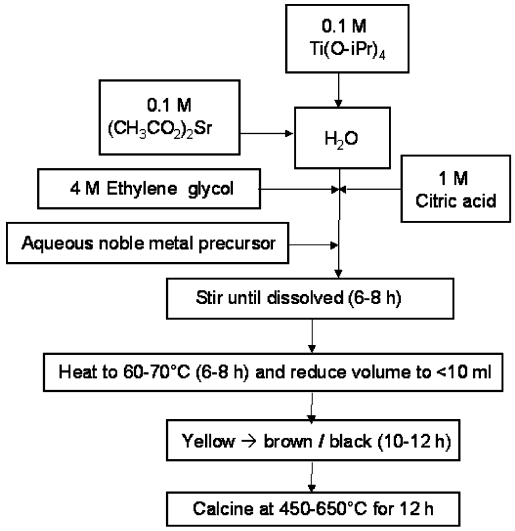

precursor in 2-propanol was added to citric acid (CA) dissolved in water. Strontium acetate was added to this solution to prepare a Sr/Ti ratio of 0.8:1, 1:1, or 1.2:1 (Scheme 1). The mixture was stirred until the solution turned transparent and clear. Ethylene glycol (EG) was added once the solution became transparent. For noble-metal-substituted $SrTiO_3$ perovskite catalyst synthesis, a solution of the metal ions, prepared from the corresponding metal salts in water, was added following the addition of the Ti and Sr precursor with EG and CA. The noble metal and strontium precursors were added stoichiometrically such that the ratio of (metal + Sr) to Ti was 1:1. The amount of noble metal added was 0.5, 1.0, or 2.0 wt % of the total weight of metal added. All precursor solutions were then stirred for another 30 min and gradually heated over 1 day to evaporate most of the water. Heating resulted in the transition of the solution from a clear liquid to a yellowish viscous paste and finally to a brown solid. The solution was thoroughly stirred until a blackish brown precipitate formed. The precipitate was calcined in air for 12 h at 400 °C, followed by an additional 12 h between 500 and 650 °C. The calcined solids were ground into a fine powder prior to characterization and photocatalytic studies. Scheme 1 shows a flowchart for the synthesis of noble-metal-substituted $SrTiO_3$ with a 1:1 Sr/Ti ratio. The same method was adapted to synthesize $SrTiO_3$ with different Sr/Ti ratios.

Characterization and Catalytic Studies. X-ray diffraction (XRD) patterns were collected for the as-synthesized powders (hereafter referred to as $SrTiO_3$, Ag−$SrTiO_3$, Pt−$SrTiO_3$, and Au−$SrTiO_3$) using Cu Kα radiation generated at 40 kV and 30 mA (X-1, Scintag Inc.). Powders were examined over 10−80° 2θ with a step size of 0.02° and step time of 0.5 s. An external standard was used for the measurement of lattice parameters. XRD peaks were fit using a Pseudo-Voigt function. Lattice parameters were determined by extrapolating measurements for the six reflections of highest 2θ versus the Nelson−Riley−Taylor−Sinclair function, using linear least-squares regression ($R^2 > 0.99$) to eliminate systematic errors.[13] Mixtures of the as-synthesized $SrTiO_3$ powder and a Ag powder (99.9%, Alfa Aesar) were prepared for known weight fractions (e.g., 0.15, 0.10, 0.05 wt % Ag, etc.). These known mixtures and the as-synthesized powders were examined more closely over 37−41° 2θ with a step size of 0.02° and a step time of 10 s.

$SrTiO_3$, Ag−$SrTiO_3$, Pt−$SrTiO_3$, and Au−$SrTiO_3$ catalyst films were cast on thin glass slides, 1.5 × 3 cm by the following procedure: A slurry of the powder was prepared in ethanol and deposited using a syringe. (10−30 wt % $SrTiO_3$ was used to prepare the slurry) The slurry was spread intermittently and allowed to dry under ambient conditions. Multiple coatings were deposited before the film was calcined for 30 min at 400 °C in air. The surface morphology of the film was imaged using atomic force microscopy (AFM) in the tapping mode (Nanoscope IIIa, Digital/Veeco Instruments). AFM was used to examine the morphology of the film with a silicon nitride tip. An ethanol solution of a dye (Victoria Blue or Acid Orange 7) was deposited on the calcined film by drop-casting the dye solution (100 μL, 10 mM) over the film and drying at room temperature. A second glass slide was placed over the catalyst films to ensure that the films were supported intact and did not lose mechanical integrity during optical measurements when they were placed over the slit of a spectrophotometer. For photocatalytic studies, the dye samples deposited on thin films of catalysts placed between the glass slides were irradiated for varying periods of time. UV−visible light was generated from a high-energy (250-W) xenon lamp, and a $CuSO_4$ solution was placed between the lamp and the catalyst film to filter high-UV emissions ($\lambda > 300$ nm). A blank spectrum (without catalyst) indicated $\lambda > 300$ nm light passing through to the other side of the cover glass. The $CuSO_4$ filter was added to prevent direct photolysis and ensure selective excitation of the TiO_2 and $SrTiO_3$ films. A UV−vis spectrophotometer (Shimadzu 3101) was used to monitor changes in the absorbance of the dye in the diffuse reflectance mode in order to estimate the extent of dye degradation.

Results and Discussion

$SrTiO_3$ Photocatalyst Synthesis. Synthesis of $SrTiO_3$ using a modified Pechini process was examined with different precursor metal salts. The catalyst obtained using strontium acetate as the precursor was found to be easier to synthesize, yielding more crystalline $SrTiO_3$ with higher purity and reproducibility, than that using a strontium carbonate ($SrCO_3$) precursor. Furthermore, $SrCO_3$ required a longer time to dissolve and occasionally led to the formation of TiO_2 following calcination. Therefore, all catalysts were subsequently prepared using strontium acetate as the precursor.

The hydrolysis of the precursor is typically much faster in an acidic medium than in an alkaline medium. This is attributed to the acid-promoted hydrolysis of the precursor wherein H ions make the alkoxide more electrophilic and thus susceptible to attack by the hydroxyl ions. $SrTiO_3$ synthesis was thus carried out at various acidic (pH adjusted using $HClO_4$) and neutral pH's to examine the influence of the extent of hydrolysis on $SrTiO_3$ synthesis. In addition to pH, the rate of addition of the catalyst precursor and water evaporation were also examined. These preparative parameters, however, were found to have little or no effect on the synthesis of the catalyst. XRD patterns for $SrTiO_3$ synthesized at pH 7 and 1.5 did not exhibit any significant differences. The only variation observed was in the time required for the solution to become transparent. At pH 7, 30 min was required for the solution to turn transparent, whereas at pH 1.5, 10 min was required. Therefore, in all subsequent syntheses, the pH of the solution was maintained at 1.5.

We also studied the effect of the calcination temperature on $SrTiO_3$. Figure 1 shows XRD patterns for $SrTiO_3$ samples calcined at 500, 550, and 650 °C for 12 h, following the preliminary heating of the photocatalyst to 400 °C for 12 h in air. As expected, the results show an increased degree of crystallization with increasing temperature. All relevant peaks

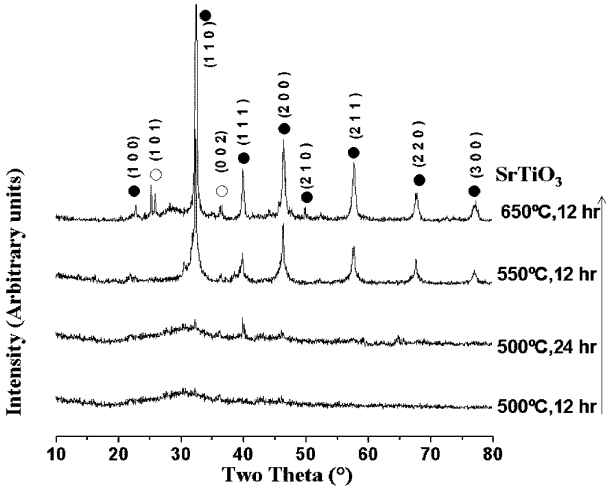

Figure 1. XRD patterns of as-synthesized $SrTiO_3$ powders prepared at different calcination temperatures.

were identified and indexed using the data available from the Joint Committee for Powder Diffraction Studies (JCPDS). $SrTiO_3$ peaks were identified using standardized data from JCPDS file 35-734 and literature results.[14] Note that small amounts of TiO_2 (JCPDS files 21-1272 and 21-1276) were also observed (Figure 1). The extent of TiO_2 formation was found to depend on the amount of water added, the duration of heating, and the calcination temperature. The optimum conditions of time and temperature for the synthesis of the perovskite were 12 h of heating at 400 °C followed by 12 h of heating in air at 550 °C.

The stoichiometry of the resulting $SrTiO_3$ depended on the Sr/Ti ratio used in the precursor composition. Kutty characterized $SrTiO_3$ with electron paramagnetic resonance (EPR) and attributed the hole-trapping ability of $SrTiO_3$ to changes in the Sr/Ti ratio.[14] A Ti-rich phase was suggested to be beneficial for hole trapping at the surface. In photocatalysis, hydroxyl-radical- (OH•) mediated oxidation of compounds can be traced to the availability of holes in the photocatalyst as

$$Sr_xTi_yO_3 + h\nu \rightarrow Sr_xTi_yO_3\,(h^+) \quad (1)$$

$$Sr_xTi_yO_3\,(h^+ + e^-) + OH^- \rightarrow Sr_xTi_yO_3\,(e^-) + OH^\bullet \quad (2)$$

where $x < y$, $x = y$, and $x > y$. Therefore, a higher hole availability at the surface under Ti-rich conditions can potentially generate higher OH• levels that can provide greater degradation rates.

Variation of the Sr/Ti ratio can therefore be expected to alter the degradation kinetics of the photocatalyst. Sr/Ti ratios were varied between 0.8:1, 1:1, and 1.2:1 because earlier studies did not show any change in the activity at closer ratios and to examine what happens to the catalytic activity if this ratio is varied beyond the formation of a single phase.

Effect of Noble Metal Doping. XRD patterns for the as-synthesized powders of $SrTiO_3$, Ag−$SrTiO_3$, Pt−$SrTiO_3$, and Au−$SrTiO_3$ with 2 wt % Ag, Pt, and Au revealed the formation of a $SrTiO_3$ solid solution, and small amounts of TiO_2, but no crystalline metal deposits were detected (Figure 2). The detection limit, for example, of Ag was determined by XRD of known mixtures to be between 0.10 and 0.05 wt % Ag. (Metal particles of comparable size were used to prepare mixtures to ensure particle sizes similar to those of the composite oxides.) The absence of reflections for the noble metals could be due to a small crystallite size, low concentration, or low crystallinity.

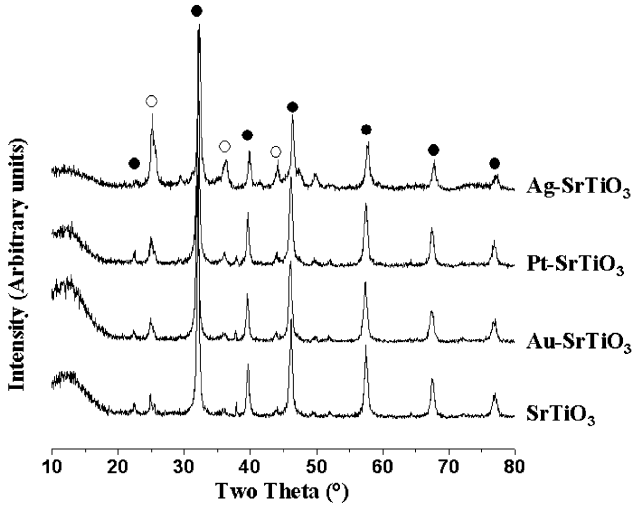

Figure 2. XRD patterns of as-synthesized powders of $SrTiO_3$ and $SrTiO_3$ prepared with 2 wt % Ag, Pt, and Au. All reflections correspond to $SrTiO_3$ or $SrTiO_3$ solid solutions (●) and TiO_2 (○).

Table 1. Lattice Parameters of the Noble-Metal−$SrTiO_3$ Powders Obtained from Figures 1 and 2

catalyst	lattice parameter
$SrTiO_3$	3.908
Au−$SrTiO_3$	3.910
Pt−$SrTiO_3$	3.913
Ag−$SrTiO_3$	3.905

Substitution of the noble metal in the perovskite structure was minimal, if it occurred at all, as shown by the measured lattice parameters (Table 1). There was only a slight increase in the lattice parameter for additions of Au and Pt. The lattice parameter measured for $SrTiO_3$ was comparable to the JCPDS standard.

Phase-pure $SrTiO_3$ was a white crystalline powder. However, the addition of noble metals Ag, Au, and Pt led to the formation of colored powders: yellow for Ag−$SrTiO_3$, pale green for Pt−$SrTiO_3$, and red for Au−$SrTiO_3$. The coloration was attributed to oxidation of the metal ions. To confirm this observation, UV−vis diffuse reflectance measurements were carried out to examine the absorption characteristics of Ag−$SrTiO_3$, Pt−$SrTiO_3$, and Au−$SrTiO_3$. Absorbance spectra showed a shift in the absorbance of $SrTiO_3$ into the visible range upon addition of Ag, Pt, and Au (Figure 3). A characteristic plasmon absorbance of the metal (e.g., Au has a plasmon absorbance at 530 nm) was observed for Au−$SrTiO_3$. This is an indication of the presence of Au in the form of Au(0). This suggests that the main portion of the 2% metal added was present as zerovalent metal. Thus, the presence of plasmon absorbance and the negligible change in the lattice parameters suggest that most of

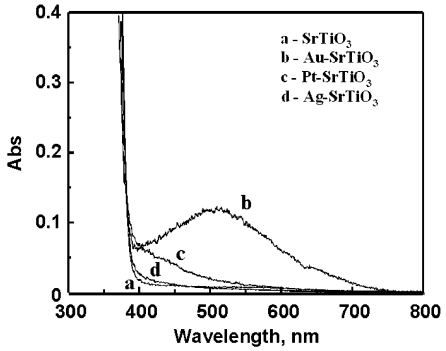

Figure 3. Absorbance spectra of (a) $SrTiO_3$ and 2 wt % (b) Au−, (c) Pt−, and (d) Ag−$SrTiO_3$.

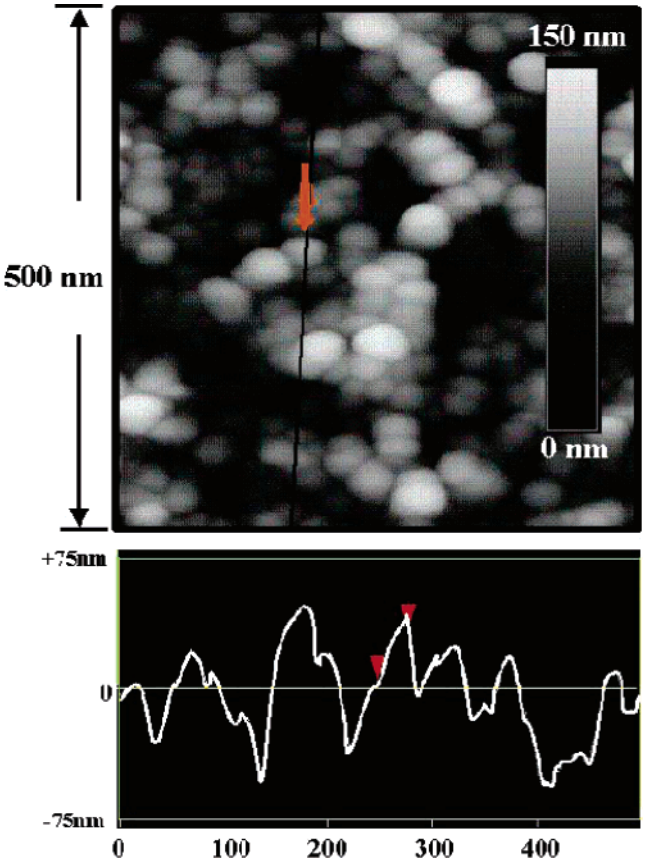

Figure 4. AFM image of a $SrTiO_3$ photocatalyst film deposited on a glass slide showing a surface image (top) and profile (bottom).

the metal exists as zerovalent metal deposits instead of substituting Sr or Ti sites within the perovskite structure. However, detailed analysis of the surface is needed to reveal the exact oxidation state of the metal and the extent of metal ion distribution.

Figure 4 shows an AFM image of a typical $SrTiO_3$ film deposited on a glass slide from a slurry of particles calcined at 550 °C. The $SrTiO_3$ films consisted of uniformly sized particles of ~50−60 nm. AFM images of films cast with particles calcined at 500 and 650 °C showed particle sizes of ~40 and ~65 nm, respectively. All films exhibited rough surfaces, implying that they are porous when viewed in cross section, and no change in particle size was observed before and after calcination at 400 °C. Films of noble-metal−$SrTiO_3$ prepared at 550 °C also showed a similar porosity and particle sizes of ~50 nm.

Photocatalytic Properties. The photocatalytic activity of $SrTiO_3$ was examined by monitoring the degradation of the dye Victoria Blue. Multiple catalyst films loaded with the dye were subjected to UV−vis degradation in air. Spectra of the dye-loaded catalyst films are shown in Figure 5. The dye showed an absorbance maximum at 560 nm. UV−vis illumination resulted in a decrease in the absorbance at 560 nm, demonstrating that catalytic degradation of the dye occurred during illumination. Blank experiments performed without any TiO_2, $SrTiO_3$, or illumination showed no change in the dye absorbance at 560 nm, indicating that the catalyst and light are essential for photocatalytic degradation. The inset in Figure 5 shows a photograph of the catalyst film before and after exposure to UV light. The complete conversion of the dye by $SrTiO_3$ occurred in the region where the catalyst was present, and no dye degradation occurred in the absence of the catalyst.

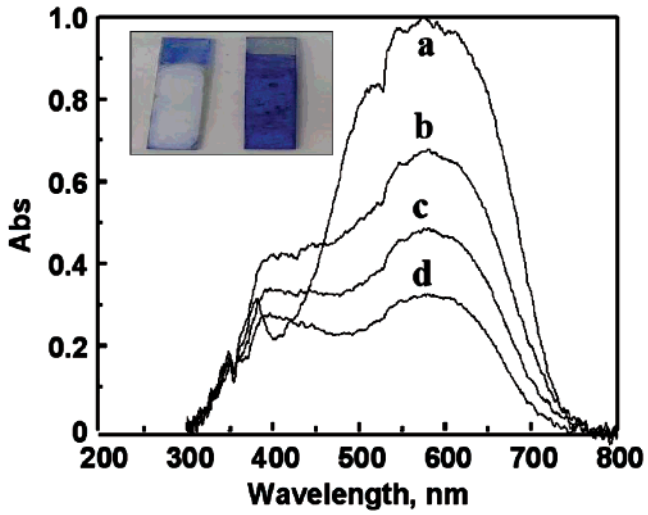

Figure 5. Absorbance spectra of a Victoria-Blue-loaded $SrTiO_3$ film following (a) 0, (b) 15, (c) 30, and (d) 60 min of UV irradiation. The inset shows photographs of the $SrTiO_3$ film containing Victoria Blue dye before (left) and after (right) UV−vis irradiation. The irradiation was carried out with a 250-W xenon lamp and with a $CuSO_4$ solution to cut off high-UV radiation (λ < 300 nm).

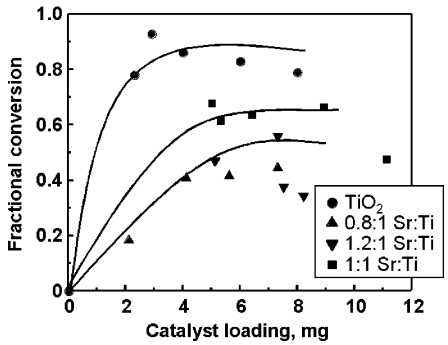

Figure 6. Comparison of the catalytic activities of TiO_2 and $SrTiO_3$ with Sr/Ti ratios of 1:1, 0.8:1, and 1.2:1. The irradiation was carried out with a 250-W xenon lamp and with a $CuSO_4$ solution to cut off high-UV radiation (λ < 300 nm).

Figure 6 shows the effect of the Sr/Ti ratio on the fractional conversion of the dye. An equimolar Sr/Ti ratio was more active for degradation of the dye than the catalysts with nonequimolar ratios. Similar results were also observed with Acid Orange 7. The photocatalytic activity of various loadings of commercially available TiO_2 (Degussa P25) was found to result in the highest conversion of Victoria Blue compared to corresponding loadings of $SrTiO_3$ (Figure 6).

Similar photocatalytic degradation rates for both TiO_2 and $SrTiO_3$ were observed in an earlier study with $SrTiO_3$.[15] Hashimoto and co-workers reported a strong oxidizing ability of holes as the cause of bleaching of Methylene Blue dye on $SrTiO_3$ films. The photocatalytic activity of $SrTiO_3$ presented here, however, is somewhat lower than that of TiO_2. The particle size of $SrTiO_3$ was ~50−60 nm, compared to 25−30 nm for TiO_2. Catalytic activity is a function of the active available surface area, which decreases with increasing particle size. Thus, the larger particle size of $SrTiO_3$ relative to TiO_2 resulted in a lower surface area and is believed to be the cause of the lower catalytic activity in the $SrTiO_3$ films used in this study.

Lower degradation was also observed in the Ti- and Sr-rich phases compared to the 1:1 Sr/Ti sample. The lower degradation in the case of the Sr-rich phase (Sr/Ti = 1.2:1), indicates lower hole availability. Under such circumstances, greater recombina-

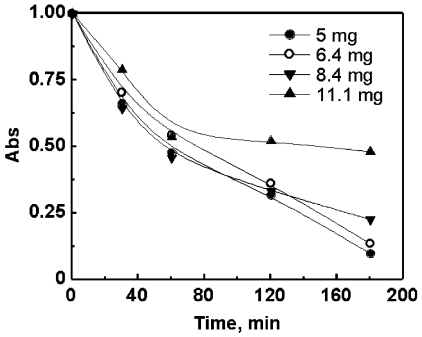

Figure 7. Effect of catalyst loading on the degradation of Victoria Blue. The absorbance at 560 nm was monitored for 3 h following different periods of irradiation. The irradiation was carried out with a 250-W xenon lamp and with a $CuSO_4$ solution to cut off high-UV radiation (λ < 300 nm).

tion between the photogenerated electron−hole pairs, because of the unavailability of excess hole centers, can indicate decreased photoactivity. On the other hand, the XRD patterns revealed that the Ti-rich catalyst contained some TiO_2. Although the Ti-rich phase is expected to provide greater numbers of surface holes, no benefits in photocatalytic dye degradation were observed. The lower activity could be attributable to the fraction of the photoactive TiO_2 in the composite. Variation of the Sr/Ti ratio between 0.95:1 and 1.05:1 also showed no change in the catalytic activity.

The amount of $SrTiO_3$ loaded in the films could also affect the photocataytic activity. The decrease in the absorbance of the dye at 560 nm following irradiation of varying amounts of $SrTiO_3$ in films (1:1 Sr/Ti ratio) at various intervals of illumination is shown in Figure 7. Increasing the film loading with $SrTiO_3$ from 5 to 8 mg did not significantly affect the dye conversion. At a higher loading of 11.1 mg, the conversion actually decreased. Because the $SrTiO_3$ films were porous and made up of spherical particles (Figure 4), it is reasonable to expect that increasing the loading would provide a greater surface area for the adsorption of the dye and increase the photocatalytic degradation. On the other hand, an increase in the film thickness with loading can attenuate light penetration, which can contribute to decreased rates of degradation at higher catalyst loadings. In our previous studies, we also observed that the degradation of Acid Orange 7 initially increased and then decreased with increased TiO_2 loading.[16,17] The kinetics of Victoria Blue degradation on $SrTiO_3$ was also examined. A preliminary estimate of the rate constant for dye conversion using a 5-mg catalyst loading was established as 0.023 min^{-1}, assuming a first-order reaction for the 5-mg catalyst loading. It is worthwhile to mention that the rate data obtained here are similar to those of a previous work (similar orders of magnitude).[17] TiO_2 and $SrTiO_3$ have similar band gaps of 3.2 eV, and hence, their photocatalytic degradation activities can be expected to be of similar orders of magnitude.

The activities of Ag−$SrTiO_3$, Pt−$SrTiO_3$, and Au−$SrTiO_3$ films were examined for the photocatalytic degradation of Victoria Blue dye under UV−visible (λ > 300 nm) and visible-light (λ > 400 nm) irradiation. The metal loadings used were 0.5, 1.0, and 2.0 wt %. Figure 8 shows a very slight change in the overall degradation of the dye under UV−visible-light irradiation over Pt−$SrTiO_3$ and Au−$SrTiO_3$ catalysts. Although the addition of noble-metal ions caused the catalyst to absorb in the visible region (as observed from the absorbance spectra), no benefits in catalytic activity were noticed.

Figure 9 shows the photocatalytic activity of Ag−$SrTiO_3$. It can be observed that there is a clear increase in the degradation

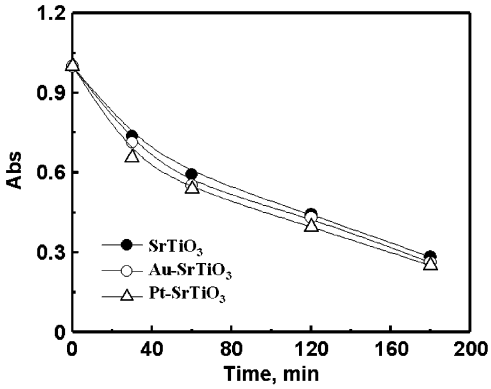

Figure 8. Changes in the absorbance at 560 nm following illumination of noble-metal−$SrTiO_3$. The absorbance at 560 nm was monitored for 3 h following different periods of irradiation with a catalyst loading of 4 mg in all cases. The irradiation was carried out with a 250-W xenon lamp and with a $CuSO_4$ solution to cut off high-UV radiation (λ < 300 nm).

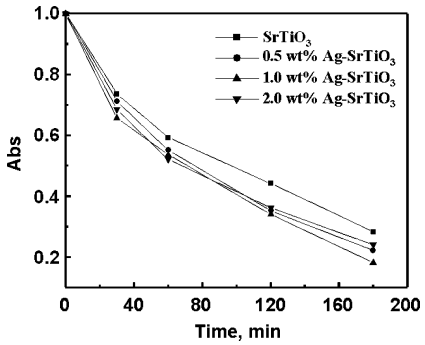

Figure 9. Changes in the absorbance at 560 nm following illumination of Ag−$SrTiO_3$ with varying Ag contents. The absorbance at 560 nm was monitored for 3 h following different periods of irradiation with a catalyst loading of 5 mg in all cases. The irradiation was carried out with a 250-W xenon lamp and with a $CuSO_4$ solution to cut off high-UV radiation (λ < 300 nm).

of Victoria Blue in the presence of Ag compared to that over plain $SrTiO_3$. Although all loadings of Ag showed higher dye conversion than plain $SrTiO_3$, the highest increase in conversion was observed for a loading of 0.1 wt %. The UV−visible-light-induced activity of Ag−$SrTiO_3$ was observed to increase the degradation of the dye by 15%.

To examine visible-light activity, the catalyst-coated dye was exposed to light at wavelengths above 400 nm. To do this, a yellow 400-nm cutoff filter (allowing blue, green, and red light only) was introduced between the $CuSO_4$ solution and the catalyst−dye-loaded glass slide. It is worthwhile to mention at this point that commercially obtained Degussa P25 and $SrTiO_3$ do not exhibit any activity toward Victoria Blue degradation when exposed to light with the 400-nm cutoff filter, showing that visible light does not cause any catalytic activity in the absence of the noble metals. Moreover, the dye degradation with visible light using Ag−$SrTiO_3$ resulted in 12% conversion, whereas no activity was observed with Pt−$SrTiO_3$ and Au−$SrTiO_3$ in the presence of the 400-nm cutoff filter. This confirmed that Ag−$SrTiO_3$ was indeed active under visible-light irradiation.

It is important to note that the noble-metal perovskites contained some TiO_2 along with $SrTiO_3$. Nonetheless, absorbance and XRD spectra of the noble-metal−$SrTiO_3$ composite showed that the metal ions were indeed deposited as zerovalent metals with possible, but extremely limited, incorporation in solid solution. This is a unique situation that, to the best of our

knowledge, has not been observed in $SrTiO_3$ photocatalysts and can be considered extremely interesting. Typically, if a metal ion were to exist in a zerovalent state over a photocatalyst ($SrTiO_3$ or TiO_2), the metal would facilitate charge separation after illumination and promote photocatalysis. Note that the plasmon absorbance at 530 nm is indicative of metal existing in the zerovalent state.[18] For example, earlier investigations involving TiO_2 doping with noble metals showed enhancement in the photoelectrochemical properties of semiconductor-based systems, which was attributed to an increase in the charge separation efficiency in the solid solution.[18] In other examples, the platinization of $SrTiO_3$ has been reported to promote water-splitting reactions.[19] In a recent study, we showed that a semiconductor−metal interface can be dynamic, wherein the metal can be oxidized by the photogenerated holes while the oxidized metal can be reduced by the electrons, resulting in an equilibrium at the interface.[16] The lack of activity enhancement in the presence of noble metals (i.e., Au and Pt) points to the possibility that the metal can act as a sink for the electrons, thereby decreasing the recombination of charges. In earlier studies, we also showed that photogenerated holes can oxidize metal ions in a solid solution.[16] Such an oxidation process will also decrease degradation of dye.

The visible-light absorbance indicates the presence of intermediate states that can facilitate the absorbance of light in the higher-wavelength region. Because the activities of the catalyst are similar in the presence of UV and visible-light illumination, we can safely rule out the possibility that Au or Pt in the metal-substituted $SrTiO_3$ structure is influencing the photocatalytic activity of the composite. Ag, however, is promising, showing ~12% enhancement in photodegradation in the presence of visible light with a Ag−$SrTiO_3$ catalyst. In an earlier report, Dzhabiev observed the formation of methane as a byproduct by photocatalytic reduction of carbon dioxide over Ag−$SrTiO_3$ composite.[20] Unlike the onset of absorbance at 400 nm for $SrTiO_3$, Ag−$SrTiO_3$ shows an absorbance tail extending to 500 nm. This visible-light absorbance could be attributed to the creation of interband states due to Ag doping inside the $SrTiO_3$ lattice and can effect photocatalytic degradation of the dye at wavelengths >400 nm.

The photocatalytic degradation reaction is a sequence of multiple elementary steps. Only a detailed study involving in situ spectroscopy and rigorous analysis of reaction products will elucidate the rate-determining step. It is worthwhile to mention that the Ag−$SrTiO_3$ catalyst holds promise in visible-light photocatalysis. To confirm further the universal applicability and the promise of this family of photocatalyst, aqueous- and gas-phase photocatalytic studies must be performed. Efforts to further characterize and optimize the Ag−$SrTiO_3$ catalyst are currently in progress.

Conclusions

$SrTiO_3$ films deposited on glass plates demonstrated photocatalytic degradation of Victoria Blue dye. A Sr/Ti ratio of 1:1 was efficient in degrading the dye compared to Sr- or Ti-rich phases. For noble-metal−$SrTiO_3$ films, catalytic activity under UV−vis illumination was found to be significant only in the presence of Ag, whereas Au and Pt showed no enhancement in photocatalytic activity when added during $SrTiO_3$ preparation. Addition of Au, Pt, and Ag resulted in the formation of zerovalent metal deposits without significant incorporation into the lattice structure. (Absorbance and XRD spectra indicated that the added metal ions were deposited as zerovalent metal species over $SrTiO_3$.) The most interesting result, however, is that Ag−$SrTiO_3$ catalysts showed a 12% enhancement in dye degradation over 180 min under UV−visible-light illumination.

Acknowledgment

This work was supported by the Office of Basic Energy Sciences of the U.S. Department of Energy. E.E.W. and V.S. acknowledge Gabriel L. Converse for assistance with quantitative XRD analysis. The assistance provided by Prof. Prashant Kamat in the form of laboratory facilities and helpful discussions is acknowledged.

Note Added after ASAP Publication. The initially approved version of this paper was published on the Web on January 11, 2006 without corrections from one of the co-authors. Several text changes have been made, and a reference has been added. The corrected version of this paper was published February 24, 2006.

Literature Cited

(1) Herrmann, J. M. Heterogeneous photocatalysis: Fundamentals and applications to the removal of various types of aqueous pollutants. *Catal. Today* **1999**, *53*, 115−129.

(2) Serpone, N.; Pelizzetti, E. *Photocatalysis. Fundamentals and Applications*; John Wiley and Sons: New York, 1989; p 650.

(3) Ollis, D. F.; Pelizzetti, E.; Serpone, N. Heterogeneous photocatalysis in the environment: Application to water purification. In *Photocatalysis. Fundamentals and Applications*; Serpone, N., Pelizzetti, E., Eds.; Wiley: New York, 1989; pp 603−637.

(4) Hwang, D. W.; Kim, H. G.; Kim, J.; Cha, K. Y.; Kim, Y. G.; Lee, J. S. Photocatalytic water splitting over highly donor-doped (110) layered perovskites. *J. Catal.* **2000**, *193*, 40−48.

(5) Mizoguchi, H.; Ueda, K.; Orita, M.; Moon, S. C.; Kajihara, K.; Hirano, M.; Hosono, H. Decomposition of water by a $CaTiO_3$ photocatalyst under UV light irradiation. *Mater. Res. Bull.* **2002**, *37*, 2401−2406.

(6) Sayama, K.; Mukasa, K.; Abe, R.; Abe, Y.; Arakawa, H. A new photocatalytic water splitting system under visible light irradiation mimicking a Z-scheme mechanism in photosynthesis. *J. Photochem. Photobiol. A: Chem.* **2002**, *148*, 71−77.

(7) Wagner, F. T.; Somorjai, G. A. Photocatalytic hydrogen production from water on Pt-free $SrTiO_3$ in alkali hydroxide solutions. *Nature* **1980**, *285*, 559−560.

(8) Zielinska, B.; Morawski, A. W. TiO_2 photocatalysts promoted by alkali metals. *Appl. Catal. B: Environ.* **2005**, *55*, 221−226.

(9) Reihl, B.; Bednorz, J. G.; Muller, K. A.; Jugnet, Y.; Landgren, G.; Morar, J. F. Electronic Structure of Strontium Titanate. *Phys. Rev. B* **1984**, *30*, 803−806.

(10) Schwartz, R. W. Chemical solution deposition of perovskite thin films. *Chem. Mater.* **1997**, *9*, 2325−2340.

(11) Kakihana, M.; Okubo, T.; Arima, M.; Uchiyama, O.; Yashima, M.; Yoshimura, M.; Nakamura, Y. Polymerized complex synthesis of perovskite lead titanate at reduced temperatures: Possible formation of heterometallic (Pb,Ti)−citric acid complex. *Chem. Mater.* **1997**, *9*, 451−456.

(12) Carp, O.; Huisman, C. L.; Reller, A. Photoinduced reactivity of titanium dioxide. *Prog. Solid State Chem.* **2004**, *32*, 33−177.

(13) Klug, H. P.; Alexander, L. E. *X-ray Diffraction Procedures*; Wiley: New York, 1974.

(14) Ahuja, S.; Kutty, T. R. N. Nanoparticles of $SrTiO_3$ prepared by gel to crystallite conversion and their photocatalytic activity in the mineralization of phenol. *J. Photochem. Photobiol. A: Chem.* **1996**, *97*, 99−107.

(15) Miyauchi, M.; Nakajima, A.; Watanabe, T.; Hashimoto, K. Photocatalysis and photoinduced hydrophilicity of various metal oxide thin films. *Chem. Mater.* **2002**, *14*, 2812−2816.

(16) Subramanian, V.; Wolf, E. E.; Kamat, P. V. Influence of metal/metal ion concentration on the photocatalytic activity of TiO_2−Au composite nanoparticles. *Langmuir* **2003**, *19*, 469−474.

(17) Subramanian, V.; Kamat, P. V.; Wolf, E. E. Mass-transfer and kinetic studies during the photocatalytic degradation of an azo dye on optically transparent electrode thin film. *Ind. Eng. Chem. Res.* **2003**, *42*, 2131−2138.

(18) Subramanian, V.; Wolf, E.; Kamat, P. V. Semiconductor−Metal Composite Nanostructures. To What Extent Do Metal Nanoparticles (Au, Pt, Ir) Improve the Photocatalytic Activity of TiO_2 Films? *J. Phys. Chem. B* **2001**, *105*, 11439−11446.

(19) Thampi, K. R.; Subba, R. M.; Schwarz, W.; Graetzel, M.; Kiwi, J. Preparation of $SrTiO_3$ by sol−gel techniques for the photoinduced production of H_2 and surface peroxides from water. *J. Chem. Soc., Faraday Trans.* **1988**, *84*, 1703−1712.

(20) Dzhabiev, T. S.; Tarasov, B. B.; Uskov, A. M. Photocatalytic Reduction of Carbon Dioxide in Aqueous Semiconductor Suspensions. *Catal. Today* **1992**, *13*, 695−696.

Received for review June 13, 2005
Revised manuscript received September 21, 2005
Accepted December 5, 2005

IE050693Y